CrossMark

*J. Fluid Mech.* (2015), *vol.* 782, *pp.* 368–379. © Cambridge University Press 2015
doi:10.1017/jfm.2015.546



# Localized turbulence structures in transitional rectangular-duct flow

**Keisuke Takeishi[1], Genta Kawahara[1,†], Hiroki Wakabayashi[1], Markus Uhlmann[2] and Alfredo Pinelli[3]**

[1]Graduate School of Engineering Science, Osaka University, Toyonaka 560-8531, Japan

[2]Institute for Hydromechanics, Karlsruhe Institute of Technology, Karlsruhe 76131, Germany

[3]School of Mathematics, Computer Science and Engineering, City University London, London EC1V 0HB, UK

(Received 12 October 2014; revised 16 July 2015; accepted 14 September 2015; first published online 8 October 2015)

Direct numerical simulations of transitional flow in a rectangular duct of cross-sectional aspect ratio $A \equiv s/h = 1$–$9$ ($s$ and $h$ being the duct half-span and half-height, respectively) have been performed in the Reynolds number range $Re \equiv u_b h/\nu = 650$–$1500$ ($u_b$ and $\nu$ being the bulk velocity and the kinematic viscosity, respectively) in order to investigate the dependence on the aspect ratio of spatially localized turbulence structures. It was observed that the lowest Reynolds number $Re_T$, estimated in a specific way, for localized (transiently sustaining) turbulence decreases monotonically from $Re_T = 730$ for $A = 1$ (square duct) with increasing aspect ratio, and for $A = 5$ it nearly attains a minimal value $Re_T \approx 670$ that is consistent with the onset Reynolds number of turbulent spots in a plane channel ($A = \infty$). Turbulent states consist of localized structures that undergo a fundamental change around $A = 4$. At $Re = Re_T$ turbulence for $A = 1$–$3$ is streamwise-localized similar to turbulent puffs in pipe flow, while for $A = 5$–$9$ turbulence at $Re = Re_T$ is also localized in the spanwise direction, similar to turbulent spots in plane channel flow. This structural change in turbulent states at $Re = Re_T$ is attributed to the exclusion of turbulence from the vicinity of the duct sidewalls in the case of a wide duct with $A \gtrsim 4$: here the friction length on the sidewalls is so long that the size (around 100 times the friction length) of a self-sustaining minimal flow unit of streamwise vortices and streaks is larger than the duct height and, therefore, it cannot be accommodated.

**Key words:** instability, transition to turbulence, turbulent flows

## 1. Introduction

A subcritical transition to turbulence can be triggered only by finite-amplitude perturbations. Since a fully nonlinear description is therefore indispensable for the transition, the elucidation of transition mechanisms and structures is much more challenging than in the case of a supercritical transition. A subcritical transition to turbulence in wall-bounded shear flows is known to be characterized in terms of

† Email address for correspondence: kawahara@me.es.osaka-u.ac.jp

https://doi.org/10.1017/jfm.2015.546 Published online by Cambridge University Press

the emergence of well-organized turbulence patches bounded by laminar regions. In circular pipe flow streamwise-localized turbulence has been observed by many investigators (see Mullin 2011). It is widely accepted that there are two kinds of localized turbulence structures, a puff and a slug (Wygnanski & Champagne 1973). Turbulent puffs appear at lower Reynolds number than slugs to play a role in the early stage of transition. At low Reynolds numbers puffs can be in an equilibrium state where they have a length of roughly 20 pipe diameters (Mullin 2011) and propagate at a speed of approximately the bulk mean velocity (Wygnanski & Champagne 1973; Nishi *et al.* 2008; de Lozar & Hof 2009). The lowest value of the onset Reynolds number (based on the pipe diameter and the bulk mean velocity) of equilibrium puffs was estimated to be 1720 by Avila, Willis & Hof (2010). In plane channel flow, on the other hand, two types of localized structures have been observed: one is a turbulent spot localized not only in the streamwise direction but also in the spanwise direction (Carlson, Widnall & Peeters 1982), and the other is a turbulent stripe localized in the direction inclined from the streamwise direction in the spanwise direction (Hashimoto *et al.* 2009). Turbulent spots first arise at lower Reynolds numbers, and as the Reynolds number increases they develop into stripes through their growth and subsequent breakup (Aida, Tsukahara & Kawaguchi 2010). Spots grow spatially in time, and their leading (or trailing) edge propagates at a speed of about 1.0–1.3 (or 0.5–0.8) bulk velocity (Carlson *et al.* 1982; Lemoult, Aider & Wesfreid 2013). An equilibrium state of spots like that of puffs has not been reported even at their onset, and equilibrium structures in a plane channel might be turbulent stripes rather than spots (Aida *et al.* 2010). The onset Reynolds number (based on channel height and bulk velocity) of spots is around 1333 (Carlson *et al.* 1982; Hashimoto *et al.* 2009).

It has recently been found that spatially localized turbulence, such as puffs and spots, appearing at relatively low Reynolds numbers is transient in the sense that turbulence will eventually decay to the laminar state (Brosa 1989; Peixinho & Mullin 2006). In phase space such localized turbulence might be considered as a non-attracting chaotic invariant set, which should be distinguished from the so-called linear transient growth, i.e. non-monotonic trajectories depending on initial conditions, in the close vicinity of the laminar state. Experimental data and numerical simulations in pipe flow have shown that the mean lifetime of turbulent puffs does not diverge at a finite Reynolds number but rather increases exponentially with the increasing Reynolds number, implying that localized turbulence in pipes is always transient, being independent of the Reynolds number (Hof *et al.* 2006; de Lozar & Hof 2009; Avila *et al.* 2010). Avila *et al.* (2011) have determined the critical Reynolds number of pipe flow as the onset Reynolds number of sustaining turbulence at which the mean lifetime of turbulent puffs before splitting is consistent with that before decaying. Above the critical Reynolds number puffs can split before their decay, so that turbulence will sustain to spread in a statistical sense.

The characteristics of a subcritical transition to turbulence in rectangular-duct flow, including the shape of localized structures, should depend on the cross-sectional aspect ratio $A$ of the duct, where $A = s/h$ ($\geqslant 1$), $s$ ($\geqslant h$) and $h$ being the duct half-span and half-height, respectively. In the case of a square duct ($A = 1$), on the one hand, the transition characteristics are believed to be similar to those of pipe flow, and the appearance of streamwise-localized structures can be expected in a turbulent state similar to turbulent puffs in a pipe. In the limit of $A \to \infty$, on the other hand, the rectangular duct becomes equivalent to a plane channel such that the transition to turbulence will resemble that of plane channel flow, and turbulence is represented by

https://doi.org/10.1017/jfm.2015.546 Published online by Cambridge University Press

streamwise- and spanwise-localized structures, i.e. turbulent spots. Now the question arises: What is the structure of localized turbulence in transitional rectangular-duct flow for finite values of $A$ larger than unity? In the present study, in order to answer this question, direct numerical simulations of rectangular-duct flow were performed at transitional Reynolds numbers using a pseudospectral method (Uhlmann *et al.* 2007; Pinelli *et al.* 2010) in a long computational domain. The lowest Reynolds number for localized turbulence is estimated in a specific way, and it is shown how the structure of turbulent states at the lowest Reynolds numbers depends on the geometrical aspect ratio of the duct. The dependence of localized turbulence structures is interpreted in the light of scaling arguments with local wall units. Finally, the structural change of localized turbulence with increasing Reynolds number is analysed.

## 2. Flow configuration and numerical simulations

We consider the motion of an incompressible viscous fluid through an infinitely long duct with a rectangular cross-section of half-height $h$ and half-span $s$ ($\geqslant h$). The fluid motion is driven by a constant flow rate $F$, and the bulk mean velocity $u_b = F/(4sh)$ is temporally invariant. A right-handed Cartesian coordinate system $(x, y, z)$ is introduced with its origin on the centre axis along which the coordinate $x$ is defined. The coordinates $y$ and $z$ are taken in the height direction and the spanwise direction, respectively. The velocity components are denoted by $u$, $v$ and $w$ along the $x$-, $y$- and $z$-directions, respectively. No-slip and impermeable conditions $u = v = w = 0$ are imposed on the duct walls, and the flow field is assumed to be periodic of length $L_x$ in the $x$-direction. The dimensionless control parameters are the Reynolds number $Re = u_b h/\nu$ and the aspect ratio $A = s/h$ ($\geqslant 1$), where $\nu$ is the kinematic viscosity of the fluid.

We solve numerically the incompressible Navier–Stokes equations with a fractional-step method (see Pinelli *et al.* (2010) for the details of the numerical method and its validation). The time integration is based on the Crank–Nicolson scheme for the viscous terms and a three-step Runge–Kutta method for the nonlinear terms including the pressure term. The flow variables are expanded in terms of truncated Fourier series in the $x$-direction and Chebyshev polynomials in the $y$- and $z$-directions. We use a collocated grid arrangement in physical space constructed from an equidistant spacing $\Delta x$ in the $x$-direction and the Chebyshev–Gauss–Lobatto points in the $y$- and $z$-directions. The nonlinear terms are evaluated in physical space whereas the explicit contribution of the linear terms is evaluated in spectral space. The fields are transformed back and forth by means of the fast Fourier transform and fast cosine transform. De-aliasing according to the 2/3 rule is performed in the $x$-direction. In numerical simulations the aspect ratio is set at $A = 1, 2, 3, 4, 5, 9$ and the Reynolds number $Re$ is varied in the range $650 \leqslant Re \leqslant 1500$. In all the simulations the streamwise period is fixed at $L_x = 40\pi h$. This is larger than the streamwise period ($32\pi$ times the pipe radius) used by Avila *et al.* (2010) in pipe-flow simulations to sufficiently avoid the interaction between leading and trailing edges of a turbulent puff that would arise in short domains.

## 3. Identifications of the lowest Reynolds number for transient turbulence

Although the onset Reynolds number of sustaining turbulence in pipes has been determined as a consequence of counteractions between the decay and splitting of turbulent puffs (Avila *et al.* 2011), the onset of sustaining turbulence in plane channels or rectangular ducts is difficult to identify. In this study, therefore, we

https://doi.org/10.1017/jfm.2015.546 Published online by Cambridge University Press

| $A$ | $Re_T$ | $Re_\tau$ | $\Delta x\, u_\tau/\nu$ | $\max(\Delta y\, u_\tau/\nu)$ | $\max(\Delta z\, u_\tau/\nu)$ |
|---|---|---|---|---|---|
| 1 | 730 | 52.5 | 6.45 | 2.58 | 2.58 |
| 2 | 710 | 48.8 | 5.99 | 2.40 | 2.40 |
| 3 | 690 | 47.3 | 5.82 | 2.33 | 2.33 |
| 4 | 685 | 45.7 | 5.61 | 2.24 | 2.24 |
| 5 | 675 | 45.6 | 5.60 | 2.24 | 2.21 |
| 9 | 670 | 46.6 | 5.72 | 2.29 | 2.57 |

TABLE 1. Simulation parameters in typical runs.

consider the lowest Reynolds number of localized transient turbulence to investigate the dependence of turbulence structures at the lowest Reynolds number on the aspect ratio of a rectangular duct.

We first identify the lowest Reynolds numbers $Re_T$ that allow transiently sustaining turbulence for $A = 1$–$9$. For each value of $A$ the Reynolds number $Re$ of the flow is gradually reduced by 5 units from $Re = 1500$, at which a fully developed turbulent state can be observed. After each reduction of $Re$ the computations are run until either the flow relaminarizes or a minimum time $900\nu/u_\tau^2$ has elapsed, where $u_\tau = \sqrt{\tau/\rho}$ is the friction velocity, $\tau$ and $\rho$ being the wall shear stress averaged over the four walls and time, and the mass density of the fluid, respectively. The sustainment of turbulence is verified at every time step by monitoring the maximum value of the (positive) second invariant $Q$ of the velocity gradient tensor (which represents vortex structures) over the whole flow field. If the maximum value of $Q(\nu/u_\tau^2)^2$ is greater than $2 \times 10^{-3}$, then the turbulence is judged to survive at that time. We measure the lowest value, $Re_L$, of the Reynolds number for the survival. For each value of the aspect ratio simulations are run with five distinct initial data, among which the minimum of $Re_L$ is identified as the lowest Reynolds number henceforth denoted as $Re_T$. It has been checked that changes in the threshold value for $Q(\nu/u_\tau^2)^2$ do not lead to a significant difference in $Re_T$. The simulation parameters in the typical runs where $Re_T$ has been identified are shown in table 1. Therein $Re_\tau = u_\tau h/\nu$ denotes the friction Reynolds number, and $\Delta y$ and $\Delta z$ are the grid intervals in the $y$- and $z$-directions, respectively.

In the present identification a relatively short duration time $900\nu/u_\tau^2$ has been taken, because localized turbulence will always decay after its finite lifetime, the probability distribution of which is exponential (Hof *et al.* 2006). If the duration time were longer, therefore, much higher values for $Re_T$ would be obtained. Near-wall turbulence is known to survive by the regeneration cycle consisting of streamwise vortices and streaks (Hamilton, Kim & Waleffe 1995), and the period of the cycle is about $282\nu/u_\tau^2$ at the Reynolds number $Re = 1333$ in the minimal flow unit ($\pi h \times 2h \times 0.35\pi h$) of plane channel turbulence (Jiménez & Moin 1991). In this study, accordingly, the duration time has been set to be short in bulk time units (say, $238h/u_b$–$292h/u_b$) but longer than the period of the near-wall regeneration cycle. A change of the duration time to $900\nu/u_\tau^2 - 400\nu/u_\tau^2$ (or $+400\nu/u_\tau^2$) was found to lead to a variation of $Re_T$ by $-2.5$ (or $+10.8$) on average. The variation of $Re_T$ with decreasing duration time is much smaller than that with increasing duration time, implying that a duration time comparable to the near-wall regeneration period would bring about a roughly consistent value of $Re_T$. This might be because the near-wall regeneration cycle would play a key role in the transient sustainment of turbulence. It should be noted that the values of $Re_T$ have been estimated in a specific way, and

https://doi.org/10.1017/jfm.2015.546 Published online by Cambridge University Press

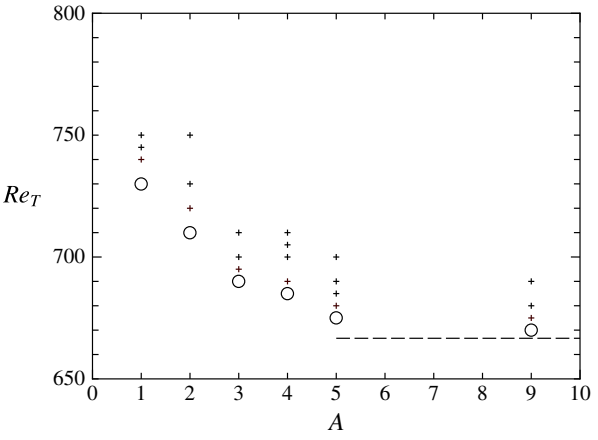



FIGURE 1. The lowest Reynolds number $Re_T$ (the minimal $Re_L$) of transient turbulence as a function of the aspect ratio $A$. The values of $Re_L$ measured in the other runs are also shown by the small symbols +. The dashed horizontal line denotes the value of $Re_T = 667$.

thus they are neither universal nor strict approximations to universal values. However, we would like to stress that localized turbulence itself can be strictly defined as a non-attracting chaotic invariant set, i.e. a chaotic saddle (Kantz & Grassberger 1985; Lai & Winslow 1995), in phase space and that the purpose of this work is to demonstrate the dependence of localized turbulence structures on the aspect ratio rather than to strictly determine their onset Reynolds number.

Figure 1 shows the dependence of the lowest Reynolds number $Re_T$ of localized turbulence on the aspect ratio $A$. The lowest Reynolds number for a square duct measures $Re_T = 730$, which is lower than the recently reported marginal Reynolds number, $Re \approx 1100$, in a square duct with minimal streamwise extension (Uhlmann *et al.* 2007). It is also lower than the onset Reynolds number (based on a pipe radius), $Re = 860$, of turbulent puffs in pipe flow (Avila *et al.* 2010). Let us define an equivalent radius of a square duct with half-height $h$ in the sense of a consistent cross-sectional area as $r = (2/\sqrt{\pi})h$; the lowest Reynolds number corresponding to pipe flow can then be expressed as $(r/h)Re_T = 824$, which is much closer to the reported value 860. It can be seen from figure 1 that $Re_T$ decreases monotonically with increasing $A$. When based on the maximum velocity of a laminar profile for a fixed bulk velocity the reduction of the lowest Reynolds number (not shown) is even more striking than that of $Re_T$ shown in figure 1. The monotonic decrease of $Re_T$ is thought intuitively to be a consequence of the weaker constraint that the sidewalls in the wider duct impose on the flow. The stabilization of infinitesimal disturbances by the sidewalls has also been found in laminar rectangular-duct flow (Tatsumi & Yoshimura 1990). For $A = 5$, however, the lowest Reynolds number nearly attains the minimal value of $Re_T \approx 670$, which is comparable to the onset Reynolds number for turbulent spots in a plane channel (Carlson *et al.* 1982; Hashimoto *et al.* 2009). Dean (1978) reported experimentally that in a fully developed turbulent state in rectangular-duct flows a skin friction coefficient is independent of the aspect ratio $A$ if $A \geqslant 7$. Although there should be a significant difference between transitional and fully turbulent flows, the effects of the sidewalls on the lowest Reynolds number of turbulence as well as the turbulent skin friction almost disappear for comparably small values of the aspect ratio $A = 5$–$7$.

https://doi.org/10.1017/jfm.2015.546 Published online by Cambridge University Press

## 4. Structures of localized turbulence

We next discuss the turbulence structures at the lowest Reynolds numbers $Re = Re_T$ for each geometrical aspect ratio. In figure 2 are shown vortex structures visualized by positive isosurfaces of the second invariant of the velocity gradient tensor. It is observed that turbulence structures exhibit spatial localization for all the values of $A$. Localized turbulence can be seen to be composed of a large number of streamwise tubular vortices. For aspect ratios close to unity ($A = 1$–$3$) there appear streamwise-localized clusters of vortical structures that are strikingly similar to turbulent puffs in pipe flow (Wygnanski & Champagne 1973). Similar to equilibrium puffs in pipe flow the localized clusters for $A = 1$–$3$ do not extend or shrink in time, and their streamwise extent is about $30h$–$40h$, which is comparable with the length of approximately 20 diameters of the equilibrium puffs (Mullin 2011). For the larger aspect ratio ($A = 4, 5, 9$), on the other hand, the vortical structures are found to disappear from the vicinity of the sidewalls ($A = 4$), and the vortical clusters are localized not only in the streamwise direction but also in the spanwise direction ($A = 5, 9$). The vortical clusters for $A = 5, 9$ will change their shape but will not fully extend in the spanwise direction. The roundish clusters for $A = 5, 9$ in figure 2 are reminiscent of turbulent spots in plane channel flow.

In the wider duct a spanwise localization of turbulence has been found in figure 2; however, the shapes of the visualized turbulence clusters depend on the threshold of isosurfaces. In order to supplement the demonstration of this crucial structural change with $A$, we shall compare turbulence intensity on the sidewalls $z/h = \pm A$ with that on the longer two walls $y/h = \pm 1$. As the typical turbulence intensity on the walls, let us take the average, $\langle \omega_{xs}^2 \rangle$ or $\langle \omega_{xl}^2 \rangle$, of the squared streamwise vorticity on the sidewalls or the longer walls. Here the average is performed over time and over the 'vigorous streamwise extent', the latter being defined as the streamwise interval in which $\langle \omega_x^2 \rangle_{yz} \geqslant \max(\langle \omega_x^2 \rangle_{yz})/2$, $\langle \cdot \rangle_{yz}$ denoting integration over the cross-plane. The turbulence intensity on the sidewalls compared with that on the other walls, $\langle \omega_{xs}^2 \rangle / \langle \omega_{xl}^2 \rangle$, is shown as a function of $A$ in figure 3. It can be seen that the relative turbulence intensity on the sidewalls attenuates with increasing $A$. It is confirmed quantitatively that the turbulence on the sidewalls significantly decays for $A = 4, 5, 9$. In the ducts of $A = 5, 9$, for which turbulent spots have been observed, the turbulence on the sidewalls has disappeared almost completely.

The expulsion of turbulence from the vicinity of the sidewalls should be a consequence of relaminarization of turbulent flow over the sidewalls rather than the other two walls. In order to inspect this aspect we consider the behaviour of the main contributor to near-wall turbulence energy production $P = -\langle u'w' \rangle \partial \langle u \rangle / \partial z|_{y/h=0}$ (with respect to the sidewall $z/h = -A$) along the sidewall bisector, where the average has been taken over time and the vigorous streamwise extent, and the prime denotes a fluctuation around the average. As shown in figure 4, the turbulence production for $A = 2$ possesses a remarkable peak of about $0.22 u_{\tau s}^4/\nu$ around $(z + s)u_{\tau s}/\nu = 12$, which corresponds to that in a plane channel, where $u_{\tau s}$ is the friction velocity averaged on the sidewall over time and the vigorous streamwise extent. This outstanding production stems from buffer-layer streamwise vortices associated with streamwise streaks on the sidewall as in a plane channel. The turbulence production, however, decreases with increasing $A$, and for $A \gtrsim 4$ there is no longer any significant production.

In their numerical simulations of plane channel turbulence Jiménez & Moin (1991) minimized the size of the periodic computational domain while sustaining turbulence activity, obtaining a minimal flow unit with a width of approximately 100 friction

https://doi.org/10.1017/jfm.2015.546 Published online by Cambridge University Press

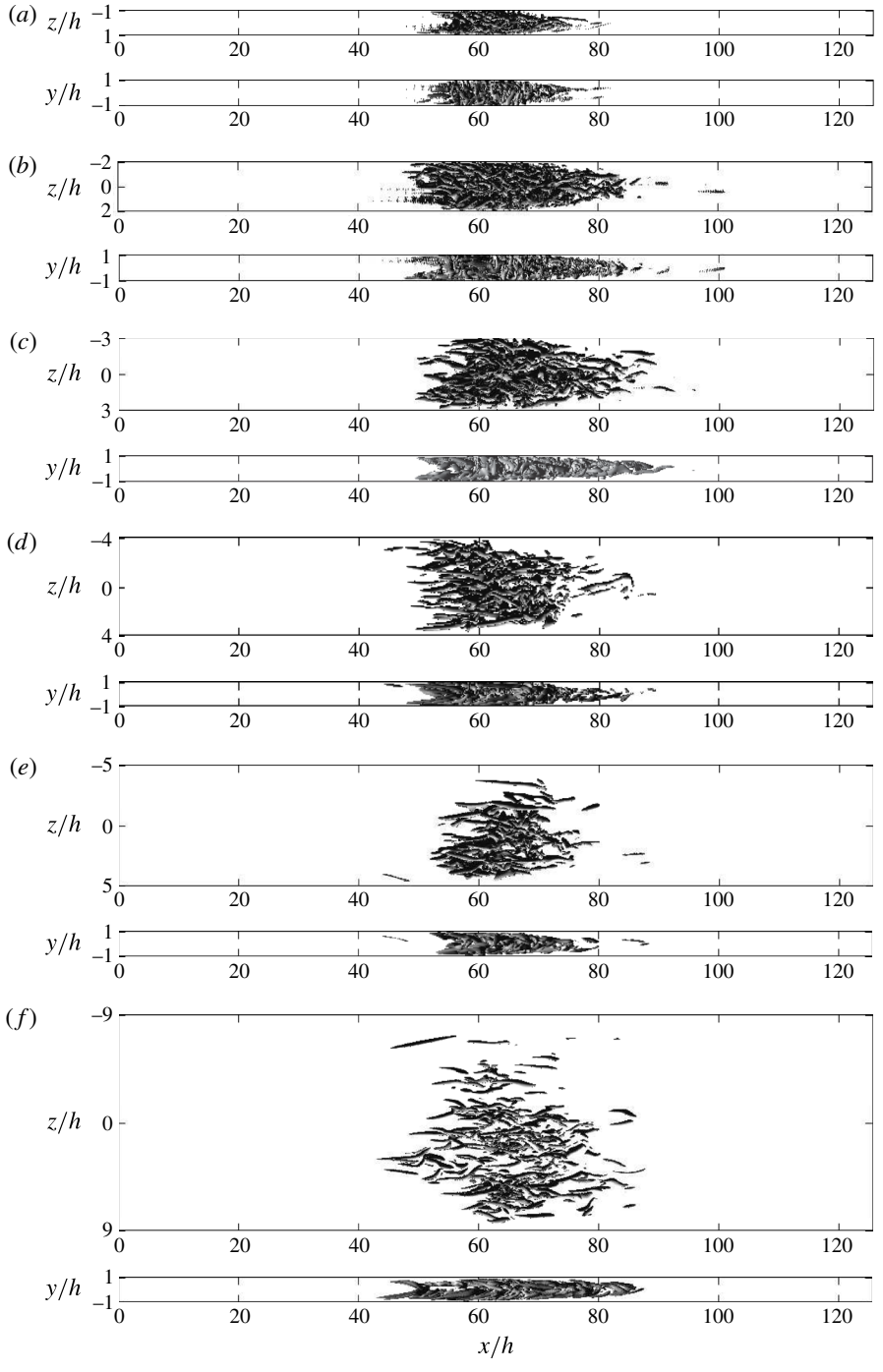



FIGURE 2. Instantaneous vortical structures visualized by isosurfaces of the second invariant of the velocity gradient tensor, $Q(\nu/u_\tau^2)^2 = 2 \times 10^{-3}$ at the lowest Reynolds numbers $Re = Re_T$ (see table 1 for the values of $Re_T$ for each $A$). (*a*) $A = 1$, (*b*) $A = 2$, (*c*) $A = 3$, (*d*) $A = 4$, (*e*) $A = 5$, (*f*) $A = 9$. All the localized structures have been centred in the $x$-direction.

https://doi.org/10.1017/jfm.2015.546 Published online by Cambridge University Press

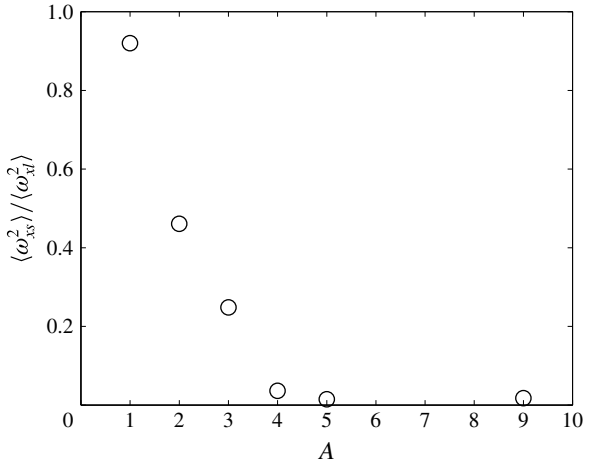



FIGURE 3. The relative turbulence intensity $\langle\omega_{xs}^2\rangle/\langle\omega_{xl}^2\rangle$ on the sidewalls as a function of $A$.

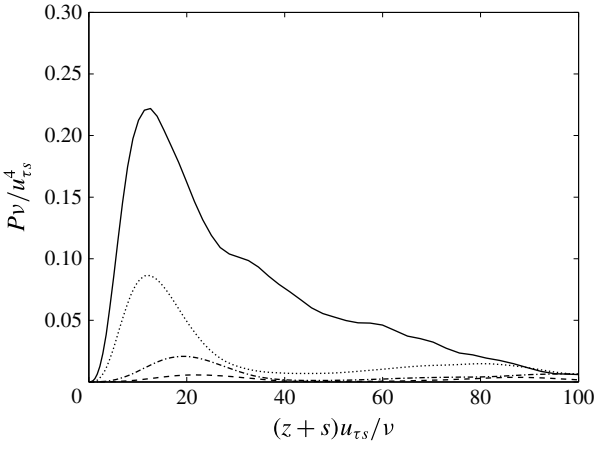



FIGURE 4. The turbulence production $P$ on the sidewall bisector $y/h=0$ as a function of the distance from the sidewall. ——, $A=2$; · · · · · ·, $A=3$; – – – – –, $A=4$; - - - -, $A=5$.

lengths, which accommodates a pair of counter-rotating staggered streamwise vortices and one low-velocity streak. If the width of the flow is less than this minimal value, turbulence dies out. Figure 5 shows the full width of the duct along the sidewall normalized with the friction length $\nu/u_{\tau s}$ as a function of $A$. It can be seen that the normalized width diminishes with increasing $A$, measuring approximately 100 for $A=2$–3. This is a direct consequence of the lower wall shear rate on the sidewalls and the greater kinematic viscosity (i.e. the increased friction length on the sidewalls) for turbulent flow in ducts of larger aspect ratio for the lower values of $Re_T$ (see figure 1). For $A \gtrsim 4$ the duct width $2h$ is smaller than 100 wall units, i.e. it cannot accommodate a minimal flow unit of near-wall turbulence. This is the reason why the flow in the vicinity of the sidewalls relaminarizes, so that the spanwise-localized spots arise for $A \gtrsim 4$. The remarkable decrease of $2h\,u_{\tau s}/\nu$ from 100 at $A=4$ in figure 5 is due to the relaminarization.

https://doi.org/10.1017/jfm.2015.546 Published online by Cambridge University Press

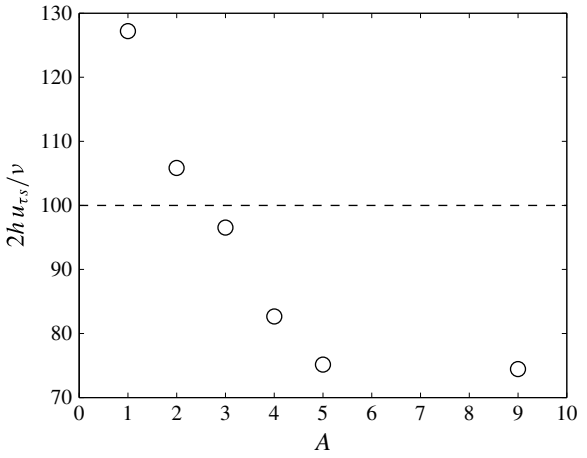



FIGURE 5. The full duct width $2h$ along the sidewall normalized with the friction length on the sidewall as a function of $A$. The dashed horizontal line corresponds to the size $100\nu/u_{\tau s}$ of a minimal flow unit in plane channel flow.

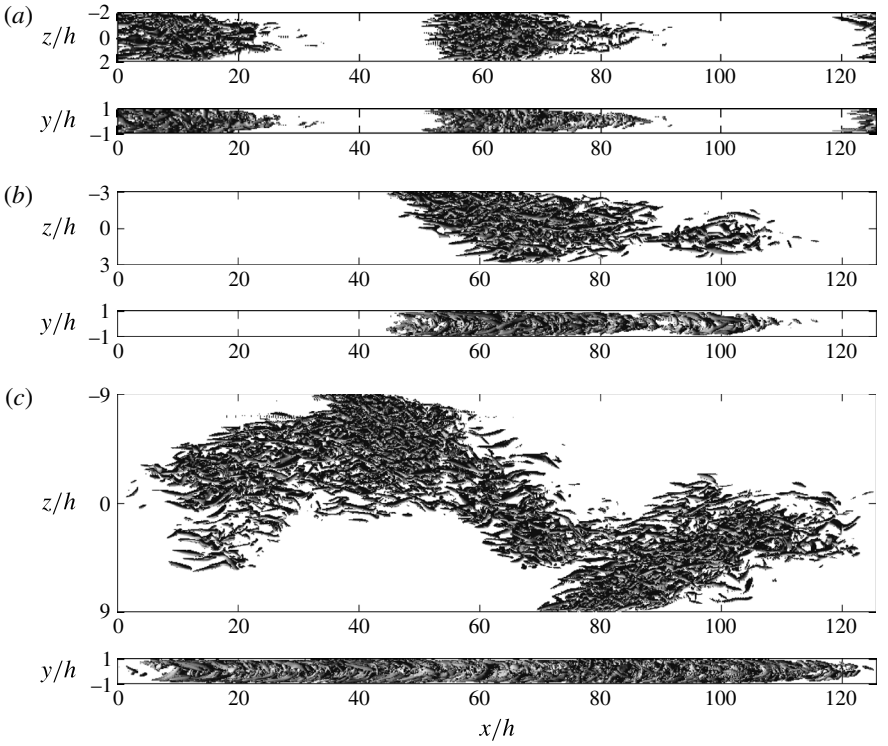



FIGURE 6. Same as figure 2 but for the higher Reynolds number $Re = 800$ than $Re_T$. (*a*) $A = 2$, (*b*) $A = 3$, (*c*) $A = 9$.

## 5. Localized turbulence structures at higher Reynolds number

In the following we briefly discuss the modifications to the localized turbulence when the Reynolds number is increased. Instantaneous vortical structures at $Re = 800$ (well above $Re_T$) are shown in figure 6. No essential difference from the turbulent

https://doi.org/10.1017/jfm.2015.546 Published online by Cambridge University Press

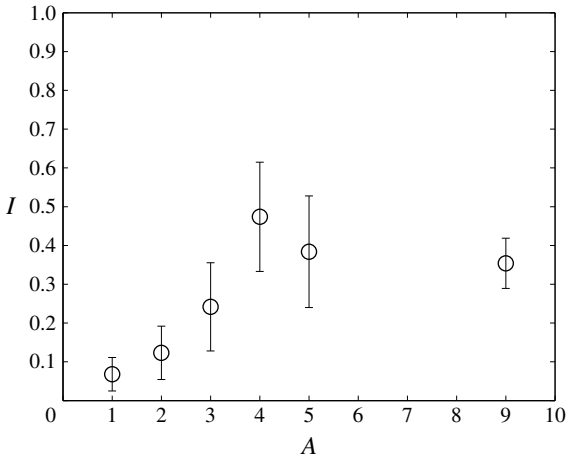



FIGURE 7. The skewness indicator $I$ of turbulence structures as a function of $A$ at $Re = 800$. The standard deviation of the skewness indicator is also shown by the vertical bars.

puff at $Re = Re_T$ can be seen in the duct with aspect ratio close to unity ($A = 2$); however, the turbulent puff in the wider duct ($A = 3$) is skewed in the spanwise direction. The meandering turbulence structures in the much wider duct for $A = 9$ are remarkably reminiscent of turbulent stripes found in plane channel flow by Hashimoto *et al.* (2009), who observed that the stripes appear in the Reynolds number range $Re = 850$–$1000$. The oblique bands in figure 6(*c*) could arise from growing spots at the higher Reynolds number, as reported in Aida *et al.* (2010).

In order to examine quantitatively the dependence on the aspect ratio of the skewness of the localized turbulence at the higher Reynolds number, a skewness indicator is introduced as follows. At a given time $t$ let us define $f(x, z, t) = \langle\omega_x^2\rangle_y / \langle\langle\omega_x^2\rangle_y\rangle_{xz}$ as a two-dimensional 'distribution function' of a vortical cluster, where $\langle\cdot\rangle_{xz}$ denotes the $(x, z)$-integration in the vigorous streamwise extent and $\langle\cdot\rangle_y$ integration over the $y$-direction. The relative coordinates $(x', z')$ with respect to the centre of the vortical cluster are then defined as $x' = x - \langle xf\rangle_{xz}$ and $z' = z - \langle zf\rangle_{xz}$. Now we compute the averaged modulus of the 'cross-correlation' of $(x', z')$ given by $I = \overline{|\langle x'z'f\rangle_{x'z'} / \sqrt{\langle x'^2 f\rangle_{x'z'} \langle z'^2 f\rangle_{x'z'}}|}$ which defines the skewness indicator $I$, where $\overline{(\cdot)}$ represents an ensemble average over 25–70 realizations for each value of $A$. In the computations the vigorous streamwise extent of a meandering cluster as in figure 6(*c*) is split into individual pieces with distinct skewness indicators. As shown in figure 7 the computed skewness of localized turbulence patches gradually increases with increasing $A$ (except for a kink at $A = 4$ which is presumably due to a statistical error), attaining a plateau for $A \gtrsim 4$.

## 6. Concluding remarks

Direct numerical simulations have been performed for transitional flow in rectangular ducts with various aspect ratios $A$. The lowest Reynolds number $Re_T$ for spatially localized (transiently sustaining) turbulence decreases monotonically from $Re_T = 730$ for a square duct with increasing $A$ due to the weakening constraint by the sidewalls in the wider duct, and for $A = 5$ it approaches the minimal value $Re_T \approx 670$, comparable to the onset Reynolds number of turbulent spots in

https://doi.org/10.1017/jfm.2015.546 Published online by Cambridge University Press

a plane channel. Turbulent states are characterized by localized structures: there appear streamwise-localized turbulent puffs for $A = 1$–3, while streamwise- and spanwise-localized turbulent spots emerge for $A = 5$–9. A puff–spot transition in localized turbulence at the lowest Reynolds numbers has been found for $A \approx 4$. The disappearance of turbulence from the vicinity of the sidewalls is responsible for this critical change of the localized structures. In the wider duct flow with $A \gtrsim 4$ the friction length on the sidewalls is so long that the span (approximately 100 friction lengths) of a self-sustaining minimal flow unit of streamwise vortices and low-velocity streaks is larger than the duct width and, therefore, it cannot be accommodated.

The phenomenological interpretation proposed in this paper of the spanwise localization of turbulence leading to turbulent spots for rectangular-duct flow should be followed by a theoretical demonstration. One candidate for a theoretical approach would be the characterization of localized structures in terms of simple invariant solutions to the Navier–Stokes equation (see Kawahara, Uhlmann & van Veen 2012). In phase space localized turbulence could be represented by a chaotic saddle (Kantz & Grassberger 1985; Lai & Winslow 1995). When there exists a chaotic saddle in phase space, trajectories originating from random initial conditions usually wander in the close vicinity of the chaotic saddle for a finite amount of time before escaping the chaotic saddle and settling into the laminar attractor. Simple invariant solutions, such as fixed points, periodic orbits and relative periodic orbits, are embedded in the chaotic saddle. The coherence of localized structures might be expressed by the embedded invariant solutions in turbulence. Since a state point in the chaotic saddle occasionally approaches the simple solutions, a good initial guess of Newton iteration for the localized invariant solutions might be extracted from localized turbulence.

Recently, a streamwise-localized relative periodic solution has been discovered in pipe flow (Avila *et al.* 2013) while a streamwise- and spanwise-localized relative periodic solution has been found in plane channel flow (Zammert & Eckhardt 2014). For a shear-driven system Brand & Gibson (2014) have discovered a streamwise- and spanwise-localized equilibrium solution in plane Couette flow. In rectangular-duct flow, to our knowledge, there are no reports of spatially localized invariant solutions; however, our own preliminary study suggests that a travelling-wave solution for $A = 1$ recently obtained by Uhlmann, Kawahara & Pinelli (2010) would exhibit the spanwise localization when tracked to $A > 1$. More recent inspection done by S. Okino (2014, private communication) implies that there would also exist a streamwise-localized travelling wave in rectangular-duct flow. These latest findings might be good starting points for a future theoretical demonstration of turbulence localization in transitional rectangular-duct flow.

**Acknowledgements**

This work was partially supported by a Grant-in-Aid for Scientific Research (grant nos 25249014, 26630055) from the Japanese Society for the Promotion of Science.

REFERENCES

AIDA, H., TSUKAHARA, T. & KAWAGUCHI, Y. 2010 DNS of turbulent spot developing into turbulent stripe in plane Poiseuille flow. In *Proceedings of ASME 2010 3rd Joint US–European Fluids Engineering Summer Meeting*, pp. 2125–2130.

AVILA, K., MOXEY, D., LOZAR, A., AVILA, M., BARKLEY, D. & HOF, B. 2011 The onset of turbulence in pipe flow. *Science* **333**, 192–196.

https://doi.org/10.1017/jfm.2015.546 Published online by Cambridge University Press

AVILA, M., MELLBOVSKY, F., ROLAND, N. & HOF, B. 2013 Streamwise-localized solutions at the onset of turbulence in pipe flow. *Phys. Rev. Lett.* **110**, 224502.

AVILA, M., WILLIS, A. P. & HOF, B. 2010 On the transient nature of localized pipe flow turbulence. *J. Fluid Mech.* **646**, 127–136.

BRAND, E. & GIBSON, J. F. 2014 A doubly localized equilibrium solution of plane Couette flow. *J. Fluid Mech.* **750**, R3.

BROSA, U. 1989 Turbulence without strange attractor. *J. Stat. Phys.* **55**, 1303–1312.

CARLSON, D., WIDNALL, S. & PEETERS, M. 1982 Flow-visualization study of transition in plane Poiseuille flow. *J. Fluid Mech.* **121**, 487–505.

DEAN, R. B. 1978 Reynolds number dependence of skin friction and other bulk flow variables in two-dimensional rectangular duct flow. *Trans. ASME J. Fluids Engng* **100**, 215–223.

HAMILTON, J. M., KIM, J. & WALEFFE, F. 1995 Regeneration mechanisms of near-wall turbulence structures. *J. Fluid Mech.* **287**, 317–348.

HASHIMOTO, S., HASOBE, A., TSUKAHARA, T., KAWAGUCHI, Y. & KAWAMURA, H. 2009 An experimental study on turbulent-stripe structure in transitional channel flow. In *Proceedings of the 6th International Symposium on Turbulence, Heat and Mass Transfer*, pp. 193–196. Begell House Inc.

HOF, B., WESTERWEEL, J., SCHNEIDER, T. M. & ECKHARDT, B. 2006 Finite lifetime of turbulence in shear flows. *Nature* **443**, 59–62.

JIMÉNEZ, J. & MOIN, P. 1991 The minimal flow unit in near-wall turbulence. *J. Fluid Mech.* **225**, 213–240.

KANTZ, H. & GRASSBERGER, P. 1985 Repellers, semi-attractors, and long-lived chaotic transients. *Physica* D **17**, 75–86.

KAWAHARA, G., UHLMANN, M. & VAN VEEN, L. 2012 The significance of simple invariant solutions in turbulent flows. *Annu. Rev. Fluid Mech.* **44**, 203–225.

LAI, Y.-C. & WINSLOW, R. L. 1995 Geometric properties of the chaotic saddle responsible for supertransients in spatiotemporal chaotic systems. *Phys. Rev. Lett.* **74**, 5208–5211.

LEMOULT, G., AIDER, J.-L. & WESFREID, J. E. 2013 Turbulent spots in a channel: large-scale flow and self-sustainability. *J. Fluid Mech.* **731**, R1.

DE LOZAR, A. & HOF, B. 2009 An experimental study of the decay of turbulent puffs in pipe flow. *Phil. Trans. R. Soc. Lond.* A **367**, 589–599.

MULLIN, T. 2011 Experimental studies of transition to turbulence in a pipe. *Annu. Rev. Fluid Mech.* **43**, 1–24.

NISHI, M., ÜNSAL, B., DURST, F. & BISWAS, G. 2008 Laminar-to-turbulent transition of pipe flows through puffs and slugs. *J. Fluid Mech.* **614**, 425–446.

PEIXINHO, J. & MULLIN, T. 2006 Decay of turbulence in pipe flow. *Phys. Rev. Lett.* **96**, 094501.

PINELLI, A., UHLMANN, M., SEKIMOTO, A. & KAWAHARA, G. 2010 Reynolds number dependence of mean flow structure in square duct turbulence. *J. Fluid Mech.* **644**, 107–122.

TATSUMI, T. & YOSHIMURA, T. 1990 Stability of the laminar flow in a rectangular duct. *J. Fluid Mech.* **212**, 437–449.

UHLMANN, M., KAWAHARA, G. & PINELLI, A. 2010 Traveling-waves consistent with turbulence-driven secondary flow in a square duct. *Phys. Fluids* **22**, 084102.

UHLMANN, M., PINELLI, A., KAWAHARA, G. & SEKIMOTO, A. 2007 Marginally turbulent flow in a square duct. *J. Fluid Mech.* **588**, 153–162.

WYGNANSKI, I. J. & CHAMPAGNE, F. H. 1973 On transition in a pipe. Part 1. The origin of puffs and slugs and the flow in a turbulent slug. *J. Fluid Mech.* **59**, 281–335.

ZAMMERT, S. & ECKHARDT, B. 2014 Streamwise and doubly-localised periodic orbits in plane Poiseuille flow. *J. Fluid Mech.* **761**, 348–359.

https://doi.org/10.1017/jfm.2015.546 Published online by Cambridge University Press